Investigation of surface pressure response of a flat plate encountering flow-induced vortices due to a cylinder

Asiye Karakus[1,2], Stephen Turnock[1], Philip Joseph[2], Chaitanya Paruchuri[2]
Maritime Engineering[1], ISVR[2], University of Southampton, Southampton SO17 1BJ UK
a.karakus@soton.ac.uk

1 Introduction

The flow generated noise for flow bluff or streamlined bodies in the flow is an important modern engineering problem. Noise -intended to be reduced- is encountered in all areas of our lives, such as air conditioners, refrigerator cooling fans, helicopter-drone propellers, ship propellers, aircraft wings and rotors, landing gears, and wind turbines. In oceans, noise pollution has increased in recent years. Unintended noise at sea can be an issue for both passengers, crew, and marine life. Prevention or reduction the noise is critical from a military perspective. Hydrodynamic noise due to turbulent flow over a lifting surface such as a propeller or hydrofoil is a flow that can be analysed theoretically and through numerical analysis methods such as computational fluid dynamics (CFD). However, it is hard to understand the complexity of the flow interaction between upstream turbulence and the sound propagation. The approach adopted here is to combine an upstream cylinder and a downstream sharp edged flat plate. There are many studies of square or circular cylinders, Dargahi (1989), Zhang et al. (2019), Cheong et al. (2008)). One step after understanding the noise is to search for new methods to reduce it. Methods to reduce noise is as important as understanding noise. Variety of implementation such as splitter plate (Duan, F., & Wang, J. (2021), Unal, M. F., & Rockwell, D. (1988), Bao, Y., & Tao, J. (2013), You et al. (1998).), detached plate (Jacob et al. (2005), Ali et al. (2012),), tandem cylinder (Geyer, T. F. (2022), Zhu et al. (2019), Liu et al. (2014), Khorrami et al. (2007).), fairings (Boorsma et al. (2009)) have been used to decrease noise both numerically and experimentally. Experimental studies can be expensive and CFD approaches can be attractive if their confidence in the quality of the predictions an that they capture the essential mechanisms for noise source generation.

The aim of this study is to understand how systematic vortices can be created for the flow around a circular cylinder and to examine the surface pressure response of a detached flat plate. The geometry and flow conditions are taken from those used experimentally by Winklet et al (2012).This paper is structured as follows. Backgroudn physics is given in Sec. II. Definition of problem geometry and numerical simulations are given in Sec. III. Then, Sec. IV discusses in detail the physical flow behaviour and radiated sound based on the numerical-simulation results. Finally, Sec. V gives the conclusions.

2 Background

The flow around a bluff body- circular cylinder in our case- will separate and become turbulent at high Reynolds Numbers-. Instabilities occur in the wake region. An example of this instability literature is known as the *von Kármán* Vortex Street. Vortex shedding from a stationary cylinder in the flow the drag and lift fluctuations on the bluff body are the main cause of noise. Dipole characteristic noise can be observed because of the drag and lift fluctuations on the body, and quadrupole characteristic noise can be observed due to unsteady wake behind the bluff body (You et al. , 1998). It is highly preferred to use a plate - as a flow controller- to disrupt the *von Kármán Vortex Street* and reduce the noise caused by vortex shedding and lift and drag fluctuations. For our study this has the advantage of also providing a vortex of known characteristic that impacts the leading edge of a flat plate. Lighthill (1952) pproposed the noise mechanism generated by a turbulent flow. In this theory Lighthill produced acoustic analogy just for a free field. After this first approach , Curle (1955) developed a general formulation for bluff body surface in fluid. Following these, Ffowcs Williams and Hawkings (FWH) (1969) generalized the formulation further for moving boundaries. Jacob et al. (2005) examined a rod-airfoil configuration in wind tunnel with low Mach number. The flow around the rod attached to the

basement and NACA-0012 has been studied, taken into account the effects of three dimensions. In the measurements made, there is a 2 mm deviation between the rod and the centre of the airfoil due to the airfoil geometry. They used two different diameters (0.01, 0.016 meter) and four different velocities for each diameter (30.5, 65, 72, 115 m/s) to understand the behaviour of flow. Strong 3-D effects, secondary vortex, vortex splitting, and stretching significantly deflect the flowfield. Due to these effects spectral broadening around the shedding frequency and its harmonics happened. As a summary, the most dominant source region is the foil leading edge where the secondary vortex is created. You et al. (1998) investigated the laminar vortex shedding behind a circular cylinder. Solutions for Re=100 and Re=160 are simulated via using unsteady 2D N-S equations for incompressible flow. Near field acoustic solutions are obtained with Curle's solution (from Lighthill analogy (1952). They compared the noise from cylinder with and without splitter plate. In low Mach numbers, main reasons for noise are lift and drag force (accordingly negligible compared to lift force). While adding a splitter plate, the vortex shedding frequency will change and accordingly the noise will decrease due to the pressure change caused by the vortex shedding. Moreover, a secondary vortex originated from plate trailing edge create reverse pressure with other vortices. Ali et al. (2012) analysed the square cylinder and plate computationally with low Reynolds Number. In their study, they investigated the effect of the gap on the pressure distribution on the plate by changing the distance between the square cylinder and the flat plate. They changed the gap between 0D and 7D and observed the critical distance in 2.3D.

Winklet et al. (2012) investigates flat plate and cylinder experimentally. In their test configuration, the gap between cylinder and plate were vary. Also, various velocity from 0 to 30 m/s with a resolution 0.3 m/s were used. Depends on the cylinder diameter and the maximum velocity the Reynolds Number about 1.7*10^4. They kept the Mach Number below 0.09. They altered the gap ratio g/d from 0 to 5 with a resolution of 0.25 mm.

3 Methodology The problem is a circular cylinder in a single-phase fluid with a freestream velocity U_∞. The Reynolds Numbers regard to the diameter and regard to the chord length are $Re_d = U_\infty * D/v$= 48000 and $Re_x = U_\infty * c/v$= 480000, respectively. A thin flat plate placed at a downstream as will be the centre axis of the cylinder and the centre axis of the flat plate are the same. The thickness of plate is D/10. The chord length of flat plate is 10D. A distance between cylinder and plate is chosen as one chord length. While upstream length of the domain is 15D, downstream of flowfield is 41D. On the vertical axis, the boundaries extend to 15D in both sides.

The left-hand side of the Fig 1 is chosen as a velocity inlet, and the right-hand side is chosen pressure outlet. On the surface of cylinder and plate slip boundary conditions are chosen for pressure to calculate to plate respond. The other surfaces (top, bottom, and faces) are chosen symmetry.
In Figure 2, a-) entire boundary mesh structure, b-) near the plate mesh refinements, c-) mesh structure around the cylinder and the wake region, and d-) the mesh refinement in the downstream area are shown respectively.

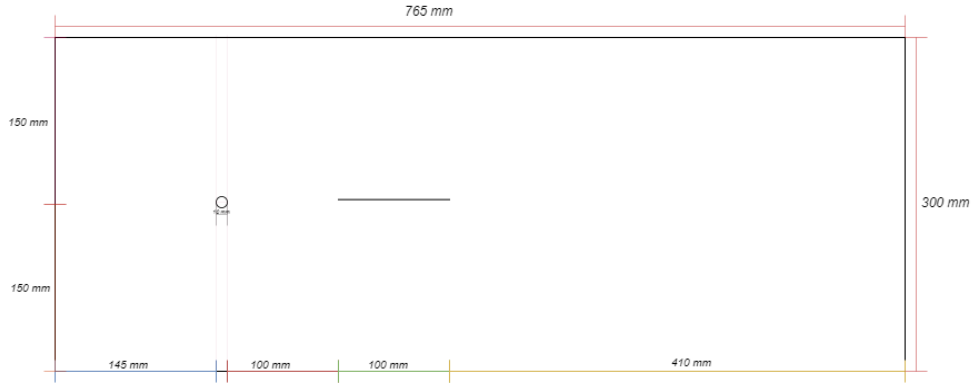

Figure 1 Computational domain

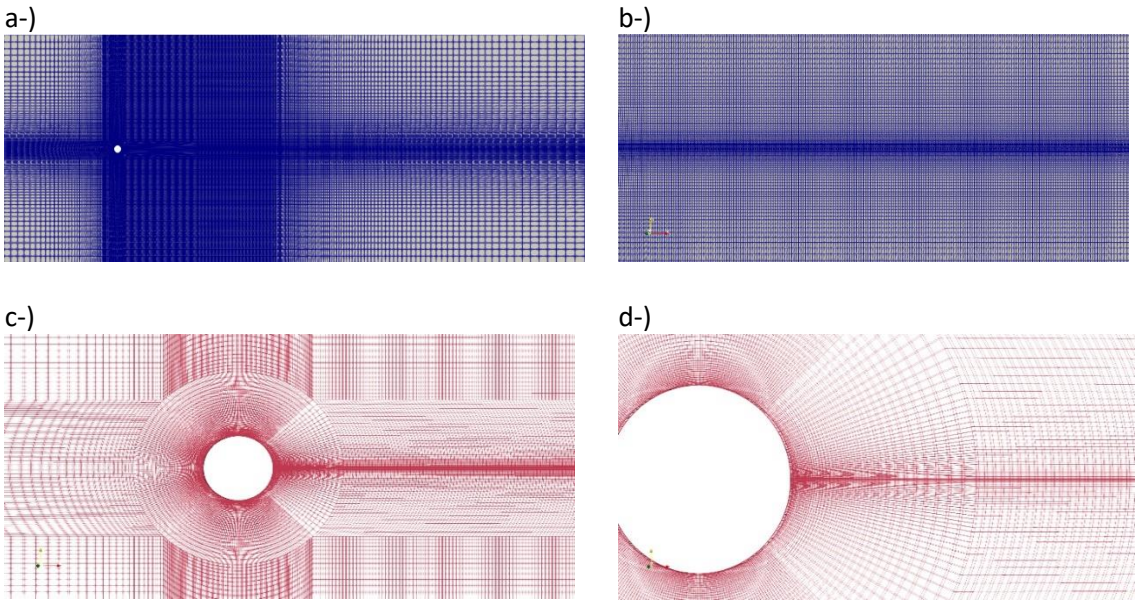

Figure 2 Mesh structure

OpenFOAM-v2006 is used for the computations(OpenFOAM | Free CFD Software | The OpenFOAM Foundation) The discretising of governing equations is done using a finite volume method. As the problem is a 2D, the blockMesh dictionary is sufficient for the mesh. Although there are minor differences around 120 000 cells is produced for each analysis. Mesh refinement is made near the cylinder and plate and the downstream of the plate (wake region). The time step size is chosen $\Delta t = 5 * 10^{-8}$ to keep the Courant Number below 0.9 dependent on the smallest cell size. Adjustable runtime is used for calculations.

The pressure values at the plate surface are calculated by solving the continuity and momentum equations in an incompressible form. The continuity equation in an incompressible form is given as:

$$\nabla . V = 0 \tag{1}$$

The momentum equation in an incompressible form is given as:

$$\rho \frac{DV}{Dt} = -\nabla P + \vartheta \nabla^2 V + F \tag{2}$$

Where, *V* is the velocity(m/s), $\nabla^2 V$ is the Reynolds stress tensor (N), *P* is the pressure (Pa), and F is the body force.

The analytical flat plate response function for a turbulent gust for high frequency and the normal incidence ($k_r = 0$) is given as:

$$g_{high}^{LE}(X, k_r = 0, k_x, M_x) = g_1(X, k_r = 0, k_x, M_x) + g_2(X, k_r = 0, k_x, M_x), \tag{3}$$

where the functions g_1 and g_2 represent the leading edge scattering and the trailing edge back-scattering of the sound, respectively.

$$g_1(X, k_r = 0, k_x, M_x) = \frac{1}{\pi\sqrt{\pi(1+M_x)k_x(b+X)}} e^{-i(\mu_a(1-M_x)\left(1+\frac{X}{b}\right)-k_x b+\frac{\pi}{4})} \tag{4}$$

$$g_2(X, k_r = 0, k_x, M_x) = \frac{(1+i)E^*\left(2\mu_a\left(1-\frac{X}{b}\right)\right)-1}{\pi\sqrt{2\pi(1+M_x)k_x b}}\, e^{-i(\mu_a(1-M_x)\left(1+\frac{X}{b}\right)-k_x b+\frac{\pi}{4})} \quad (5)$$

where X is distance from the leading edge, M_x is Mach number, k_r and k_x are turbulent wave numbers, b is half chord length, μ_a is acoustic reduced frequency and E^* is the conjugate of the Fresnel integral. (Blandeau, 2011)

4 Results

Pressure fluctuations are given at Figure 3 at the leading edge and at downstream on plate. As can be seen in the figure, at the leading edge because of the stagnation point pressure does not represent a regular sinusoidal wave. There is a remarkable difference between negative and positive sides with the different pattern. The pressure fluctuation is periodic but still not equal on the upper and bottom surface of the plate very near to the leading edge, this is shown in the figure 3/b.

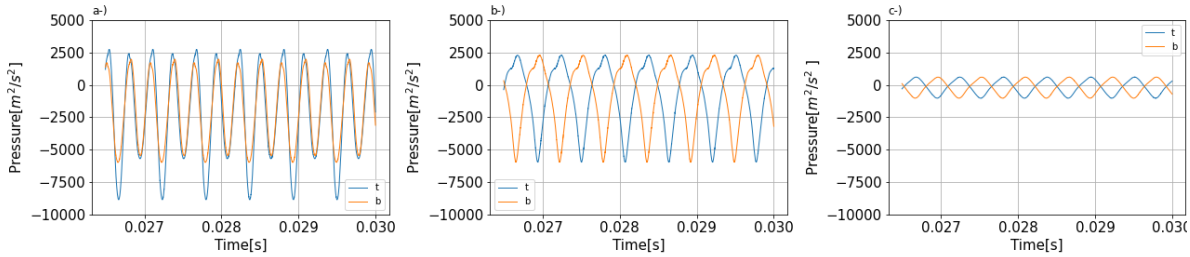

Figure 3. a-) leading edge pressure (x/c=0) and b-) very near to the leading edge (x/c=0.01) c-) downstream pressure on plate (x/c=0.25), t is upper surface and b is bottom surface of the plate.

The sound caused by the pressure difference between the surfaces of plate is shown in Figure 4. At the leading edge, max peak of sound pressure level is in the different frequency from other positions. Max noise occurs just around the 3556 Hz. The leading edge follows different pattern compared to downstream. As seen in Figure 4/b at the first peak max value of Sound Pressure Level (SPL) is 51.19 dB. The second highest peak is approximately 17 dB lower. (34.55 dB) The highest peak at the same frequency as the leading edge in the downstream region (can be seen in figure 4/c) is 38.26 dB. Similarly, the second highest peak is only in order of 14 dB (14.21 dB).

For each place apart from the leading edge itself, the highest peak can be seen at the same frequency which is 1778 Hz. Reduced frequency is 0.247.

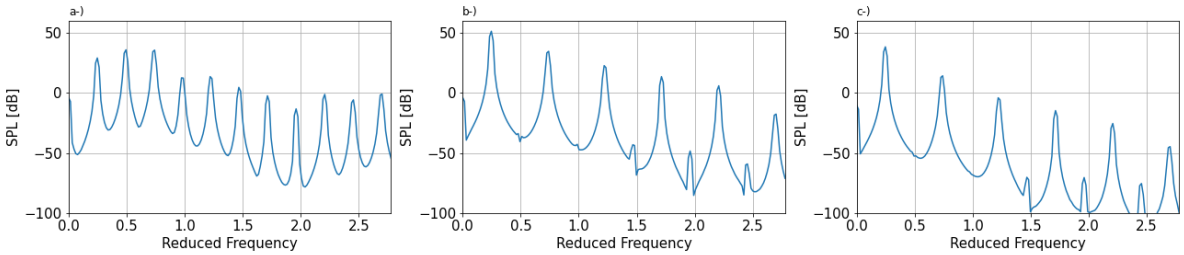

Figure 4. a-) leading edge sound pressure level between upper surface and bottom surface of plate and b-) is very near to the leading edge and c-) is downstream sound pressure level from pressure differences between upper and bottom surface

The overall sound pressure level based on distance is compared to the flat plate respond from Amiet formulation (1975) by using same conditions. As can be seen in figure 5. Although the general trend is the same as for the Amiet formulation, fluctuations are observed on the plate in the computational solution.

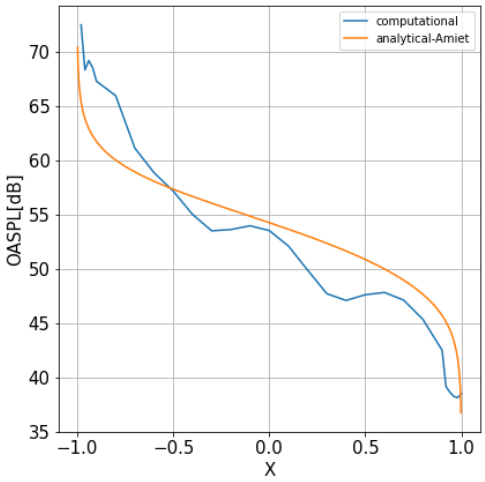

Figure 5 Plate responds compared to analytical solution, Amiet(1975).

The encounter of the plate with the incoming vortices at different times and the vortices formed on the leading edge are shown in figure 6.

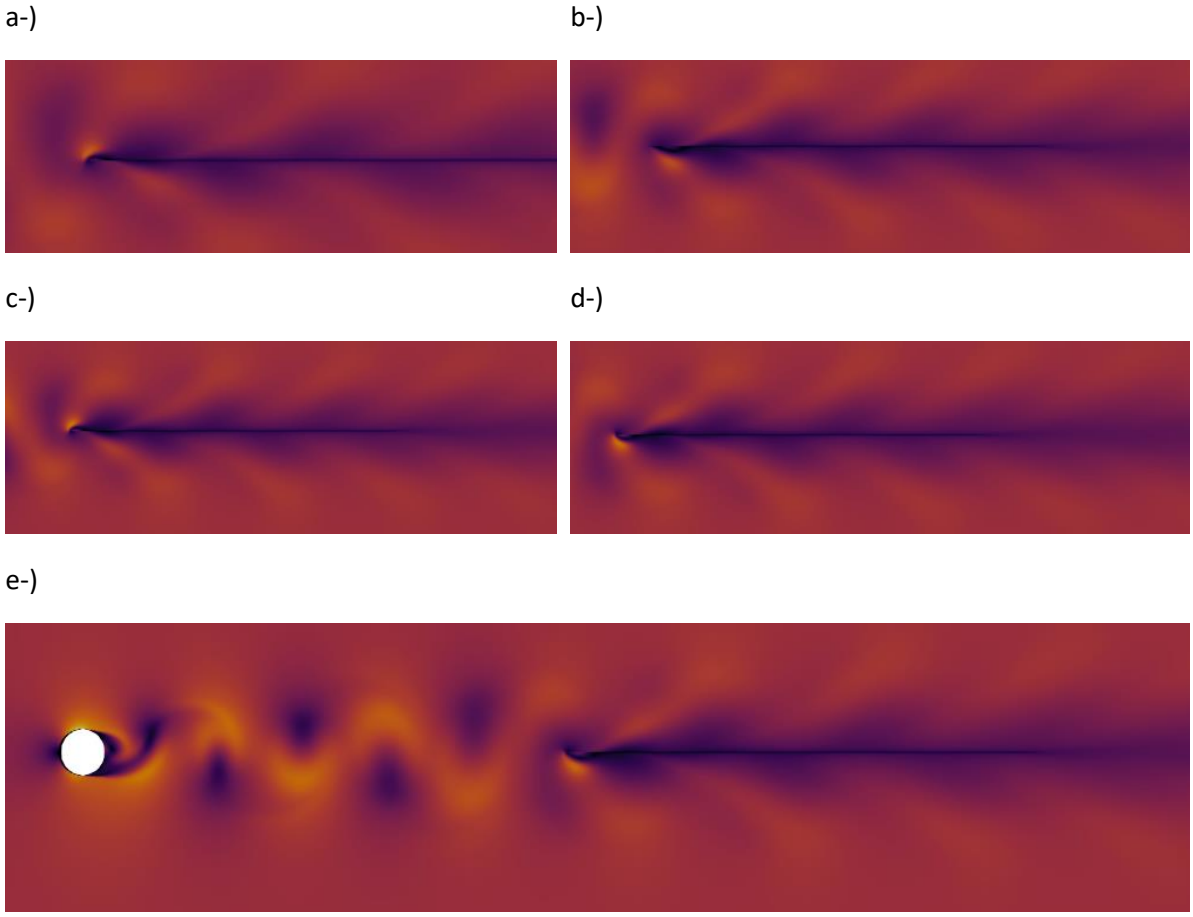

Figure 6 Vortex shedding at different times a-) t=0.015 s, b-) t=0.02 s, c-) t=0.023 s, d-) t=0.025 s, e-) t=0.029 s, respectively.

5 Conclusion

In this study, flow around a cylinder-plate combination has been solved in uniform flow using incompressible viscous solver. Numerical hydroacoustic results have been compared to analytical

solution of plate respond. Hydrodynamic information at the leading edge and trailing edge of the flat plate has not been fully captured due to coarse mesh. Although the mesh has been refined near boundaries, the finer mesh should be used for a more accurate solution. The focus of future work will be on improving mesh design and using 3D mesh. Therefore, by using 3D mesh the edge effect can be observed. Furthermore, to accurately capture plate response for both incompressible and compressible flow, other unsteady methods such as large-eddy simulation will be required.

Acknowledgements
We would like to thank the Ministry of Education in Turkey who has supported Asiye Karakus for her Ph.D. studies.

References
Cheong, C., Joseph, P., Park, Y., & Lee, S. (2008). Computation of aeolian tone from a circular cylinder using source models. Applied Acoustics, 69(2), 110-126.
Dargahi, B. (1989). The turbulent flow field around a circular cylinder. *Experiments in fluids*, *8*(1), 1-12.
Zhang, C., Moreau, S., & Sanjosé, M. (2019). Turbulent flow and noise sources on a circular cylinder in the critical regime. AIP Advances, 9(8), 085009.
Jacob, M. C., Boudet, J., Casalino, D., & Michard, M. (2005). A rod-airfoil experiment as a benchmark for broadband noise modeling. Theoretical and Computational Fluid Dynamics, 19(3), 171-196.
You, D., Choi, H., Choi, M. R., & Kang, S. H. (1998). Control of flow-induced noise behind a circular cylinder using splitter plates. AIAA journal, 36(11), 1961-1967.
Winkler, M., Becker, K., Doolan, C., Kameier, F., & Paschereit, C. O. (2012). Aeroacoustic effects of a cylinder-plate configuration. AIAA journal, 50(7), 1614-1620.
Ali, M. S. M., Doolan, C. J., & Wheatley, V. (2012). Low Reynolds number flow over a square cylinder with a detached flat plate. International Journal of Heat and Fluid Flow, 36, 133-141.
Zhu, W., Xiao, Z., & Fu, S. (2019). Simulations of turbulence screens for flow and noise control in tandem cylinders. Red, 105, 1.
Liu, H., Azarpeyvand, M., Ilario da Silva, C. R., & Wei, J. (2014). Tandem cylinder flow and noise control. In 20th AIAA/CEAS Aeroacoustics Conference (p. 3294).
Geyer, T. F. (2022). Experimental Investigation of Flow and Noise Control by Porous Coated Tandem Cylinder Configurations. AIAA Journal, 1-12.
Khorrami, M. R., Choudhari, M. M., Lockard, D. P., Jenkins, L. N., & McGinley, C. B. (2007). Unsteady flowfield around tandem cylinders as prototype component interaction in airframe noise. AIAA journal, 45(8), 1930-1941.
Boorsma, K., Zhang, X., Molin, N., & Chow, L. C. (2009). Bluff body noise control using perforated fairings. AIAA journal, 47(1), 33-43.
Duan, F., & Wang, J. (2021). Fluid–structure–sound interaction in noise reduction of a circular cylinder with flexible splitter plate. Journal of Fluid Mechanics, 920.
Unal, M. F., & Rockwell, D. (1988). On vortex formation from a cylinder. Part 2. Control by splitter-plate interference. Journal of Fluid Mechanics, 190, 513-529.
Bao, Y., & Tao, J. (2013). The passive control of wake flow behind a circular cylinder by parallel dual plates. Journal of Fluids and Structures, 37, 201-219.
Blandeau, V. (2011). *Aerodynamic broadband noise from contra-rotating open rotors* (Doctoral dissertation, University of Southampton).
Amiet, R. K. (1975). Acoustic radiation from an airfoil in a turbulent stream. *Journal of Sound and vibration*, *41*(4), 407-420.